





# The application of coal mining waste to the production of construction ceramics: radiological and mechanical aspects

 M. Bonczyk<sup>a</sup> ,  J. Rubin<sup>b</sup>

a. Central Mining Institute, Department of Environmental Radioactivity, (Katowice, Poland)  
b. Silesian University of Technology, Department of Building Process and Building Physics, (Gliwice, Poland)  
 [mbonczyk@gig.eu](mailto:mbonczyk@gig.eu)

Received 28 February 2022

Accepted 26 July 2022

Available on line 18 October 2022

**ABSTRACT:** The article presents the results of research on the physical and radiological properties of building ceramics made of mining waste. One method of using mining waste is to use it as aggregate in road construction. However, this alone is not enough to dispose of the entire amount of waste generated. Another promising method of using mining waste is the production of building ceramics (bricks). However, some properties (e.g. the content of natural radionuclides) of the waste may limit the possibility of such use. In the scope of this work, the properties of bricks made from mining waste - shale collected from dumps, were examined. It has been shown that the properties of bricks prepared in this way meet the criteria set out in various standards and legal acts and can be used in construction.

**KEY WORDS:** NORM; Mining waste; Ceramics; Radioactivity.

**Citation/Citar como:** Bonczyk, M.; Rubin, J. (2022) The application of coal mining waste to the production of construction ceramics – radiological and mechanical aspects. *Mater. Construcc.* 72 [348], e300. <https://doi.org/10.3989/mc.2022.01822>.

**RESUMEN:** *Aplicación de los residuos de la minería del carbón en la producción de cerámica de construcción: aspectos radiológicos y mecánicos.* El artículo presenta los resultados de una investigación sobre las propiedades físicas y radiológicas de la cerámica de construcción a partir de residuos mineros. Los desechos de la minería se pueden emplear como áridos en la construcción de carreteras. Sin embargo, esto por sí solo no es suficiente para eliminar la totalidad de los residuos generados. Otro método prometedor para utilizar los desechos mineros es la producción de cerámica para la construcción (ladrillos). Sin embargo, algunas propiedades (p. ej., el contenido de radionucleidos naturales) de los desechos pueden limitar la posibilidad de dicho uso. En el ámbito de este trabajo se examinaron las propiedades de los ladrillos fabricados a partir de residuos mineros - esquistos recogidos de vertederos. Se ha demostrado que las propiedades de los ladrillos preparados así cumplen los criterios establecidos en diversas normas y documentos legales, y pueden utilizarse para la construcción.

**PALABRAS CLAVE:** NORM; Residuos mineros; Cerámica; Radiactividad.

**Copyright:** ©2022 CSIC. This is an open-access article distributed under the terms of the Creative Commons Attribution 4.0 International (CC BY 4.0) License.

## 1. INTRODUCTION

Waste accompanies all human activities, especially in industrial ones. One of the most environmentally burdensome industries is hard coal mining due to the generation of large amounts of waste. It is estimated that around 60 million tons of mining waste are generated annually across the world (1).

Inappropriate management of this waste may cause the degradation of the natural environment. The waste from hard coal mining accumulated in landfills is a considerable burden for the local natural environment. The scale and extent of this phenomenon depends on many factors, including the amount and type of the waste, as well as its chemical composition and the content of heavy metals, the concentration of natural radionuclides, radon exhalation and other physical properties (2).

In addition to the aspects related to environmental protection, the economic aspect is also important which is related to the process of storing the waste and the resulting financial burden.

Some of the waste, due to its properties, can be used in the construction industry (3-4), e.g. in the production of construction ceramics (5-8). For instance the waste from glass wool industry can be used to porous ceramics production (9-10). The following mining wastes may be used in the construction ceramics industry (11):

- 1) hard coal processing waste, including shale and self-burned shale;
- 2) tailings from rock mining.

Shale is one of the components of gangue obtained in the extraction of hard coal and it is stored in dumps. The coal extraction and separation process does not have ideal efficiency and therefore a certain amount of coal is stored in dumps along with waste rocks. This situation can lead to self-ignition which will initiate thermal activity. High temperatures may change some physical properties of shale. Additionally, a dump with shale poses a potential risk to the environment due to the possibility of sulfides leaching, which contaminate groundwater and soil. Thermally active dumps emit significant amounts of CO and CO<sub>2</sub> (12-14).

Mining waste can be used in ceramic production as a component of ceramic masses (11, 15, 16). Self-burned shale – waste from mining industry, due to its chemical and mineralogical composition, is similar to brick clay. Its physical properties are also similar to brick clay. It can be classified as sintering materials and can therefore be useful for the production of ceramic products (11).

A significant problem with the proposed mining waste management is the varied content of natural radionuclides, e.g. <sup>226</sup>Ra, <sup>232</sup>Th and <sup>40</sup>K, present in investigated wastes. The research (11) carried out on 24 samples of shale collected from 13 dumps in the area of the Upper Silesian Coal Basin show

the variability of the concentration of the above radionuclides: <sup>226</sup>Ra (52.7 – 367 Bq·kg<sup>-1</sup>), <sup>232</sup>Th (3.5 – 106 Bq·kg<sup>-1</sup>), <sup>40</sup>K (241 – 892 Bq·kg<sup>-1</sup>).

The permissible limit for the concentration of natural radionuclides in construction materials which reach the trading standards set by the European Union is regulated by the EURATOM 2013/59 Directive (17). The maximum concentration of radium <sup>226</sup>Ra, thorium <sup>232</sup>Th and potassium <sup>40</sup>K is determined by the following formula (Equation [1]):

$$\frac{C_{Ra}}{300 \text{ Bq}\cdot\text{kg}^{-1}} + \frac{C_{Th}}{200 \text{ Bq}\cdot\text{kg}^{-1}} + \frac{C_K}{3000 \text{ Bq}\cdot\text{kg}^{-1}} < 1 \quad [1]$$

where  $C_{Ra}$ ,  $C_{Th}$  and  $C_K$  mean the activity concentration of <sup>226</sup>Ra, <sup>232</sup>Th and <sup>40</sup>K, respectively (expressed in Bq·kg<sup>-1</sup>).

The expression is used to ensure that annual effective dose for people, does not exceed 1 mSv if such material is used to construction the model room, according to the following scenario:

Dimensions of the model room: 4 x 5 x 2.8 m.

Thickness and density of the structures: 20 cm, 2350 kg·m<sup>-3</sup>.

Annual exposure time: 7000 hours.

Another aspect related to natural radioactivity is the exhalation of radon <sup>222</sup>Rn from ceramic blocks produced from mining waste. Radon is a noble gas, a product of radioactive decay of <sup>226</sup>Ra. It can migrate in the pore space and get out of the block (exhalation). However, the exhalation rate depends not only on the concentration of the parent isotope – <sup>226</sup>Ra, but also on the porosity and permeability of the material. Directive EURATOM 2013/59 (17) introduces the reference level of radon concentration in air in buildings of 300 Bq·m<sup>-3</sup>. The construction materials should not result in the increase of radon concentration in rooms above this limit.

In the scope of this study, the possibility of using shale from one of the Upper Silesian Coal Basin dumps as the basic raw material in the production of construction ceramics was investigated. Three ceramic samples (cylindrical bricks) were prepared. The samples were sintered in three various temperatures in order to verify the influence of this parameter to mechanical and radiological properties. Subsequently, the basic mechanical properties of sintered bricks were tested. The radioactivity content and radon exhalation rate were also examined.

## 2. MATERIALS AND METHODS

### 2.1 Study area

This work focuses on mining waste generated in the Upper Silesian Coal Basin, Poland (Figure 1). This is an area where the industry has been dominated by

coal mining for almost 200 years. The management of the generated waste is a very important issue for this region. Approximately, 30 million tons of waste from hard coal mining is generated in Poland annually and 600 million tons was deposited in Poland – accumulated in landfills, dumps and sediment ponds (16).



FIGURE 1. The location of the investigated mining area – the Upper Silesian Coal Basin, Poland.

## 2.2 Preparation of ceramic samples

Ceramic samples (cylinders) were prepared from self-burned shale and brick clay. The self-burned shale was grinded before ceramic mass preparation. The amount of technological water was determined experimentally. The forming by the vibration method in cylindrical molds with the following dimensions: height = diameter = 8 cm was applied. The industrial methods of brick shaping were not applied due to preliminary and experimental character of this work.

The final composition of the ceramic mixture is presented in Table 1.

TABLE 1. The composition of the tested ceramic mixture.

No.	Component:	Unit:	Per 1 m <sup>3</sup> of mixture (weight percentage):
1.	Grinded shale from dump (fr. 0÷0.5 mm)	[kg]	897.1 (51.9%)
2.	Birck clay (fr. 0÷0.5 mm)	[kg]	384.4 (22.2%)
3.	Water	[kg]	448.5 (25.9%)
Total:		[kg]	1730.0 (100%)

Sintering of the formed and dried samples was carried out at temperatures of 900°C, 1000°C and 1100°C, named CL\_900, CL\_1000 and CL\_1100, respectively. The duration of the burning cycle was 10-11 hours (in the electric furnace chamber), and cooling within 13-14 hours.

The samples did not show any cracks, scratches or visible deformations. Only in the case of samples prepared at 1100 °C was there a significant volume contraction.

## 2.3 The determination of physical and chemical parameters of bricks

In the scope of this work the following parameters were determined: Absolute density (pycnometric method), bulk density (directly, based on regular shape of samples), open and total porosity (based on density measurements), water absorption (capillary method), static compressive strength (for cylindrical samples in a dried state according to the standard EN 772-1:2011+A1:2015-10 Methods of test for masonry units. Part 1: Determination of compressive strength) and softening coefficient (decrease in compressive strength of the material under the influence of water).

The ceramic elements are classified to the strength class by determined normalized compressive strength factor, according to EN 771-1:2011+A1:2015-10 Requirements for masonry elements. Part 1: Ceramic masonry elements.

Analysis of the mineral composition of the raw material was carried out by the XRD method (Phillips PW-1040 analyzer, in the 2θ measuring range 5-70°).

Additionally, the permeability of one brick was determined. This factor controls the radon exhalation rate (described in chapter 2.3). Permeability is the ability of a solid to allow liquid or gas to pass through it. Quantitatively, it is expressed as permeability coefficient  $K_p$ , in millidarcy – mD.

The permeability of the ceramic sample was measured using Pressure Decay Profile Permeameter PDPK-400 (CoreLab). Tests were made for the cylindrical ceramic sample, parallel and perpendicular to the axis of the core. Tests were held using a gas (nitrogen) at the temperature of 20 °C penetrating and passing through the sample at the measurement point. The permeability was determined based on the time curve of gas pressure decrease (18). The equipment used enables standard measurements of sample permeability for gas and tests including the effect of gas slip (19) so that even at low speeds, the gas flowing through the porous material behaves in accordance with Darcy's law. The obtained permeability coefficient can also be converted into filtration coefficient ( $k$ ) for water (expressed in m/s) using the Equation [2]:

$$k = K_p \frac{\gamma}{\eta} \quad [2]$$

where:

$K_p$  is the permeability coefficient (mD),  $\gamma$  is the specific gravity of liquid (N/cm<sup>3</sup>) and  $\eta$  is the dynamic viscosity of liquid (Pa·s).

## 2.4 Radiological characterization

### 2.4.1 Gamma-ray spectrometry

The activity concentration of the following radionuclides  $^{238}\text{U}$ ,  $^{235}\text{U}$ ,  $^{226}\text{Ra}$ ,  $^{228}\text{Ra}$ ,  $^{228}\text{Th}$ ,  $^{210}\text{Pb}$  and  $^{40}\text{K}$  was determined using a gamma-ray spectrometry equipped with a hyper purity germanium detector (HPGe) with relative efficiency of 35%, cooled by liquid nitrogen ( $\text{LN}_2$ ). The energy calibration was performed using a multi-gamma source which contains isotopes ( $^{226}\text{Ra}$ ,  $^{214}\text{Bi}$ ,  $^{214}\text{Pb}$ ,  $^{210}\text{Pb}$ ,  $^{228}\text{Ac}$ ,  $^{212}\text{Pb}$ ,  $^{208}\text{Tl}$ ), emitting gamma lines in a wide range (46 – 2600 keV). Specialized software, LABSOCS by Canberra, was applied to perform efficiency calibration. It relies on the Monte Carlo simulation model which is based on the characteristics of detector and sample (chemical composition, dimensions, etc). This approach enabled the non-destructive measurement of the samples which were also investigated in radon exhalation experiments. The samples were tested in their original shape – a cylinder of height 8 cm and 8 cm in diameter (the dimensions could be affected by contraction which occurred after brick firing). The samples were covered with radon leakage proof aluminum foil in order to reach radioactive secular equilibrium between radium and radon progeny. The mathematical model has been validated by the use of certified reference materials (CRM) containing natural radionuclides – RGU-1, RGTh-1 and RGK-1 provided by the International Atomic Energy Agency (IAEA). The LabSOCS calculates the density correction factor and the same model can be applied to samples with different density. The software calculates all the correction factors related to cascade coincidence summing (CCS). The following energy lines were used in activity concentration determination:  $^{238}\text{U}$  was determined via  $^{234}\text{Th}$  (63 keV) and  $^{234\text{m}}\text{Pa}$  (1001 keV);  $^{235}\text{U}$  was determined directly (144 and 163 keV) and additionally via line interfering with  $^{226}\text{Ra}$  (186 keV);  $^{226}\text{Ra}$  was determined via radon progeny  $^{214}\text{Bi}$  (609, 1120 and 1765 keV) and  $^{214}\text{Pb}$  (295 and 352 keV) after a 3-week waiting period in order to reach secular equilibrium between radium and radon progeny;  $^{228}\text{Ra}$  was determined via  $^{228}\text{Ac}$  (911 keV);  $^{228}\text{Th}$  was determined via  $^{212}\text{Pb}$  (239 keV) and  $^{208}\text{Tl}$  (583 keV) – the appropriate correction for series branching was applied;  $^{210}\text{Pb}$  and  $^{40}\text{K}$  were determined directly based on 47 and 1461 keV, respectively.

Based on the results of the gamma-ray spectrometry, the activity index  $I$  was calculated according to Equation [1]. Activity index was introduced in the report of the European Commission – Radiation protection 112 and Directive EURATOM 2013/59. One element in Equation [1] –  $^{232}\text{Th}$  cannot be determined by gamma-ray spectrometry directly due to the lack of significant gamma lines in the spectra.

However, in the case of secular radioactive equilibrium,  $^{232}\text{Th}$  may be determined via its progeny – e.g.  $^{228}\text{Ac}$  or  $^{212}\text{Pb}$ . In such a situation, the progeny isotopes concentration may be assigned to the primordial isotope.

### 2.4.2 Radon exhalation rate determination

The radon  $^{222}\text{Rn}$  exhalation rate of the tested samples was determined. The measurement of the radon exhalation rate was performed using the closed chamber method (CCM). This method is commonly used for the measurement of the radon exhalation rate of building materials. A similar method was used in investigations performed by Leonardi *et al.* (19). A cylindrical exhalation chamber of  $60\text{ dm}^3$  was used. The thickness of the chamber's steel walls is 5 mm. Active monitor of radon concentration – AlphaGuard equipped with an open ionization chamber and the tested sample was placed inside the chamber, closed and sealed. Effective chamber volume when taking into account the presence of AlphaGuard and sample is  $55.5\text{ dm}^3$ . In the experiments, the samples, previously measured with gamma-ray spectrometry, were tested. The measurement time was about 7 days per sample. A 1-hour period in diffusion mode (without pumping) was applied. After the experiment, the results were transferred from the device to a PC and analyzed.

In CCM, radon concentration in the accumulation chamber is related to the radon exhalation rate of the sample enclosed in it. In particular, radon concentration built up  $C(t)$  inside the chamber is modeled by two-dimensional diffusion theory, according to Sahoo (20) and can be expressed by the following formula:

$$C(t) = C_0 + C_m(1 - e^{-\lambda t}) \quad [3]$$

$$C_m = \frac{E \cdot S}{\lambda \cdot V_{\text{eff}}} \quad [4]$$

Where,

$E$  = radon exhalation rate ( $\text{Bq m}^{-2} \text{h}^{-1}$ )

$S$  = surface of sample exposed in the chamber ( $\text{m}^2$ )

$V_{\text{eff}}$  = volume of accumulation chamber – [volume of AlphaGuard + volume of the sample] ( $\text{m}^3$ )

$\lambda$  = effective decay constant of radon ( $\text{h}^{-1}$ )

$C_0$ ,  $C_m$  = radon concentration in the accumulation chamber at time=0 and the maximum value ( $\text{Bq} \cdot \text{m}^{-3}$ ).

Starting from equation 3-4, the data was plotted and fitted in MS Excel using an exponential function and Solver algorithm (see results shown in Figure 2). The parameter achieved from the best fit and used to calculate the radon exhalation rate according to eq. 3 is  $C_m$ . Then,  $E$  is calculated according to Equation [5]:

$$E = C_m \frac{\lambda \cdot V_{\text{eff}}}{S} \quad [5]$$

### 3. RESULTS AND DISCUSSION

#### 3.1 Physical and chemical parameters of components used in brick preparation

The results of the chemical and physical analysis of the tested raw materials – shale and brick clay, two components used in the preparation of bricks, is shown in Table 2.

TABLE 2. Chemical and physical properties of shale and brick clay - components used for brick preparation.

No.	Parameter	unit	shale	brick clay
1	Chemical composition	SiO <sub>2</sub>	53.70	60.94
		Al <sub>2</sub> O <sub>3</sub>	16.00	16.20
		Fe <sub>2</sub> O <sub>3</sub>	9.30	8.88
		CaO	5.60	3.97
		MgO	3.30	1.34
		SO <sub>3</sub>	2.20	0.27
		Other:	3.70	1.88
2	Loss on ignition (1000°C)	% (mass)	6.20	6.52
3	Density	g·cm <sup>-3</sup>	2.72	2.77
4	Particle size distribution	mm	0 ÷ 0.5	0 ÷ 0.5
5	Radioactivity	<sup>40</sup> K	795	444
		<sup>226</sup> Ra	139	35.0
		<sup>232</sup> Th	81	40.0

The chemical/mineralogical composition of the investigated shale does not differ significantly in comparison to conventional brick clay. The biggest differences are visible in the case of radionuclide content. The concentration of <sup>40</sup>K, <sup>226</sup>Ra and <sup>232</sup>Th in shale is significantly higher than in brick clay.

#### 3.2 Physical parameters of bricks

The prepared cylindrical bricks (3 sample) were tested in order to determine major physical properties. The results are shown in Table 3.

The total volume of pores and the surface of pores decreases as the burning temperature rises. However, density and relative porosity seem to be unaffected by burning temperature. In the case of sample CL\_1100, significant volume contraction was observed. It is reflected also in such parameters as total porosity, water absorption and compressive strength, which is significantly higher in comparison to CL-900 and CL\_1000. The lack of alkali elements in used shale is probable reason of poor compressive

TABLE 3. Physical properties of shale and clay used in the experiment.

No.	Physical property	unit	Sample		
			CL_900	CL_1000	CL_1100
1.	Total volume of pores, V <sub>ep</sub>	mm <sup>3</sup> ·g <sup>-1</sup>	159	111	99.3
2.	Surface of pores, F <sub>wp</sub>	m <sup>2</sup> ·g <sup>-1</sup>	0.30	0.10	0.08
3.	Average radius of pores, P <sub>p</sub>	nm	1232	1559	2497
4.	Relative porosity (open), P <sub>w</sub>	%	17.46	17.61	18.06
5.	Absolute density	g·cm <sup>-3</sup>	2.9	2.8	2.8
6.	Bulk density	g·cm <sup>-3</sup>	1.5	1.4	1.9
7.	Total porosity, P <sub>bw</sub>	%	47.9	48.9	31.2
8.	Water absorption by weight, n <sub>w</sub>	%	29.0	28.5	20.5
9.	Normalized compressive strength, f <sub>c</sub>	MPa	7.0	6.4	21.3
10.	Coefficient of softening,	-	0.88	0.87	0.80
11.	Permeability, K	mD	-	41.5	-
12.	Filtration coefficient, k	m·s <sup>-1</sup>	-	3.9·10 <sup>-7</sup>	-

strength of bricks prepared in temperature below 1100°C. The most important change is visible in the case of compressive strength. The brick prepared in 1100°C is characterized by compressive strength of 21.3 MPa. It is a value which is comparable with results obtained for conventional construction bricks. The ceramic elements are classified to the strength class by determined normalized compressive strength factor. The prepared bricks CL\_1100 can be classified to the 20th class of compressive strength. The permeability and filtration coefficient were determined only for one type of brick (CL\_1000) prepared in 1000°C as an example.

Important property of bricks prepared from waste is leachability of some elements. Such experiments were out of scope this investigation, however they

should be done in future. The results of such tests can help to understand how mobile are toxic or potentially toxic elements present in brick, e.g. radionuclides.

### 3.3 Radioactivity of the bricks

The results of gamma-ray spectrometry analysis are shown in Table 4. The comparable radionuclide content levels for all three samples were observed. No (anti)correlation between firing temperature and the content of volatile radionuclide (e.g.  $^{210}\text{Pb}$ ) was observed. The radioactive equilibrium between  $^{238}\text{U}$ ,  $^{226}\text{Ra}$  and  $^{210}\text{Pb}$  was observed. Activity Concentration Index I was calculated according to the requirements of European Directive EURATOM 2013/59. This parameter indicates the radiation hazard related to external exposure to gamma radiation. In European countries, the activity index limit is set as 1.0, which means that such material does not create enhanced radiation exposure – there is very low probability of absorbing a radiation dose higher than 1 mSv per year. Such material may be used without any limitations. In the case of  $I > 1.0$  there is need for deeper analysis of radiation hazard related to the usage of such material.

According to Equation [1], the  $^{232}\text{Th}$  activity concentration should be taken into consideration. Because it is not possible to measure the concentration of this radionuclide on gamma-ray spectrometry directly, its progeny concentration has to be considered. The secular equilibrium between  $^{228}\text{Ra}$  ( $^{228}\text{Ac}$ ) and  $^{228}\text{Th}$  is visible in the tested samples. As a result, an assumption can be made that progeny concentrations reflect the concentration of parent radionuclide -  $^{232}\text{Th}$ . The arithmetic mean of  $^{232}\text{Th}$  decay products concentrations

TABLE 4. The results of gamma-ray spectrometry analysis (the total expanded uncertainties  $k=2$  are given).

Radionuclide	Sample code		
	CL-900	CL-1000	CL-1100
	Bq·kg <sup>-1</sup>		
$^{238}\text{U}$	101 ± 32	114 ± 35	119 ± 27
$^{226}\text{Ra}$	108 ± 14	111 ± 13	108 ± 12
$^{210}\text{Pb}$	104 ± 31	115 ± 34	106 ± 32
$^{228}\text{Ra}$	69.8 ± 4.8	70.3 ± 4.8	70.1 ± 4.7
$^{228}\text{Th}$	71.2 ± 6.6	72.2 ± 6.7	71.5 ± 6.7
$^{235}\text{U}$	5.3 ± 1.5	4.9 ± 1.4	6.8 ± 1.5
$^{40}\text{K}$	684 ± 61	693 ± 62	695 ± 62
Activity Index I	0.94	0.96	0.95

was considered in the final calculations of activity concentration index I.

The value of activity concentration index I, calculated for examined samples does not exceed 1, however it is relatively high. It is caused by elevated radionuclides concentration observed in used mining waste – shale. Final index value can be controlled by changing of proportion of shale and brick clay used as components of prepared ceramic mass.

In all cases, the value of activity index did not exceed 1. Dose criterion is not exceeded for the usage of such materials in bulk amounts as well as superficial materials.

### 3.4 Radon exhalation rate

The next property of construction materials, which is important from a radiological point of view, is the radon exhalation rate. Figure 2 shows

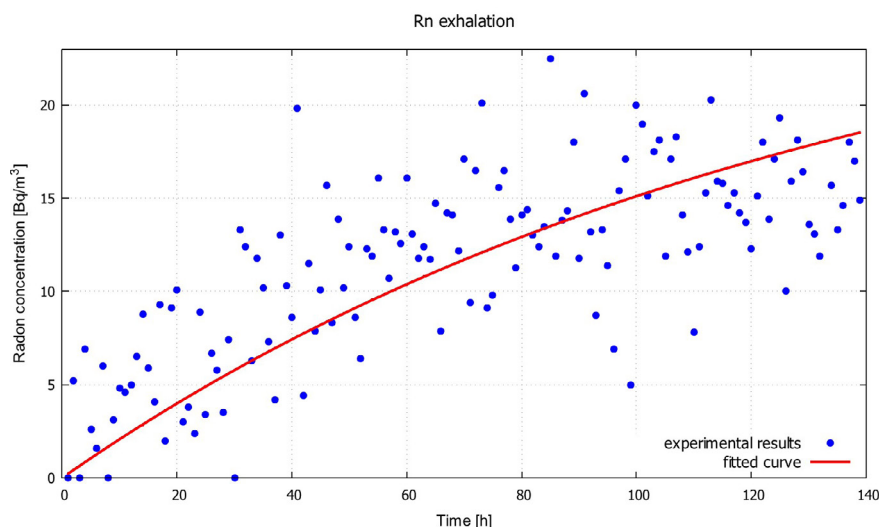


FIGURE 2. Growth of radon concentration in the exhalation chamber – sample CL\_1000.

TABLE 5. Radon exhalation rate parameters.

Parameter	Sample code		
	CL_900	CL_1000	CL_1100
$C_m$ [Bq·m <sup>-3</sup> ]	28.1 ± 5.9	28.5 ± 5.4	27.9 ± 6.1
$E$ [Bq·m <sup>-2</sup> ·h <sup>-1</sup> ]	0.38 ± 0.08	0.39 ± 0.08	0.38 ± 0.08

the growth of <sup>222</sup>Rn concentration in the exhalation chamber during a 140-hour experiment. The parameters and exhalation rates for the tested samples are shown in Table 5.

The function expressed by Equation [3] was fitted to the experimental points. The initial radon concentration  $C_0$  was taken as zero. The saturation concentration  $C_m$  was estimated based on the fitted curve. The radon exhalation rate was calculated according to Equation [4].

The observed radon concentration in the exhalation chamber is low. Due to this, the data points are compromised due to high uncertainty – approximately 20% (uncertainty is not marked in the chart in Figure 2). As a consequence, the final uncertainties of the estimated parameters are also relatively high. Nevertheless, the observed exhalation – in all samples – is low. The measured radon exhalation rate of concrete prepared with the use of some industrial waste, reported by Leonardi et al. (19), varied from 1.2 to 14.9 Bq·m<sup>-2</sup>·h<sup>-1</sup>. Despite the elevated radium <sup>226</sup>Ra (parent of <sup>222</sup>Rn) concentration and moderate permeability, the radon exhalation rate measured in tested bricks is low. The elevated radiation exposure related to radon exhalation is not expected.

#### 4. CONCLUSIONS

In the scope of this work, ceramic bricks were prepared using mining waste – shale collected from dumps. The physical and chemical properties of raw materials and prepared ceramic elements were tested. Tested properties of bricks, such as density, porosity and compressive strength, indicate significant similarity to conventional construction ceramics. However, the influence of burning temperature on the physical properties of bricks, such as compressive strength, is noticeable. The closest similarity to conventional ceramics is observed in the case of the bricks burned at 1100°C. The lack of alkali elements in used shale is probable reason of poor compressive strength of bricks prepared in temperature below 1100°C. Prepared bricks can be classified to the 20th class of compressive strength according to EN 771-1:2011+A1:2015-10 Requirements for masonry elements. Part 1: Ceramic masonry elements. Also, the highest values of other functional parameters were observed in the case of the highest burning temperature. Using a waste or clay containing more

alkali elements can improve mechanical parameters of bricks fired in temp. 900-1000°C.

The leachability of some elements should be tested, however the authors did not have capabilities to perform such experiment. Nevertheless, the result of leaching experiment could help to understand how the elements are bounded in the brick structure.

The burning temperature did not influence radionuclide content in bricks. The reduction of radionuclide concentration during the firing of bricks was not observed. There was no difference (in the range of measurement uncertainty) among the bricks prepared at each temperature. In each case, the activity index  $I$  did not exceed the limit value. As a result, there is no limitation in the use of such bricks in residential construction. Despite the relatively high concentration of <sup>226</sup>Ra and moderate permeability, the measured radon exhalation rate  $E$  is very low. This may be caused due to the formation of a tight shell around the radium-containing grains during the burning process. Such a shell reduces radon migration to pore space (emanation) and results in low exhalation rate. However, this explanation requires separate research.

Due to the advantageous physical and chemical parameters of ceramics made from mining waste, the recommendation of this method waste recycling is justified.

#### ACKNOWLEDGEMENTS

Authors would like to thank Mr Przemysław Smalec MSc, for performing tests of mechanical properties of bricks. This work was supported by the Ministry of Science and Higher Education, Poland [11158010].

#### AUTHOR CONTRIBUTIONS:

Conceptualization: M. Bonczyk. Data curation: M. Bonczyk, J. Rubin. Formal analysis: M. Bonczyk. Investigation: M. Bonczyk, J. Rubin. Methodology: M. Bonczyk. Resources: M. Bonczyk, J. Rubin. Visualization: M. Bonczyk. Writing - original draft: M. Bonczyk. Writing - review & editing: J. Rubin.

#### REFERENCES

1. Murmu, A.L.; Patel, A. (2018) Towards sustainable bricks production: An overview. *Constr. Build. Mater.* 165, 112–125. <https://doi.org/10.1016/j.conbuildmat.2018.01.038>.
2. Puertas, F.; Suárez-Navarro, J.A.; Alonso, M.M.; Gasco, C. (2021) NORM waste, cements, and concretes. A review. *Mater. Construcc.* 71 [244], e259. <https://doi.org/10.3989/mc.2021.13520>.
3. Subashi De Silva, G.H.M.J.; Hansamali, E. (2019) Eco-friendly fired clay bricks incorporated with porcelain ceramic sludge. *Constr. Build. Mater.* 228, 116754 <https://doi.org/10.1016/j.conbuildmat.2019.116754>.
4. Kusiorowski, R.; Zaremba, T.; Piotrowski, J. (2014) The potential use of cement-asbestos waste in the ceramic masses destined for sintered wall clay brick manufacture. *Ceram. Int.* 40, 11995–12002, <https://doi.org/10.1016/j.ceramint.2014.04.037>.

5. Luo, L.; Li, K.; Fu, W.; Liu, C.; Yang, S. (2020) Preparation, characteristics and mechanisms of the composite sintered bricks produced from shale, sewage sludge, coal gangue powder and iron ore tailings. *Constr. Build. Mater.* 232, 117250. <https://doi.org/10.1016/j.conbuildmat.2019.117250>.
6. Lemougna, P.N.; Yliniemi, J.; Ismailov, A.; Levanen, E.; Tanskanen, P.; Kinnunen, P.; Roning, J.; Illikainen, M. (2019) Recycling lithium mine tailings in the production of low temperature (700–900 °C) ceramics: Effect of ladle slag and sodium compounds on the processing and final properties. *Constr. Build. Mater.* 221, 332–344. <https://doi.org/10.1016/j.conbuildmat.2019.06.078>.
7. Stolboushkin, A.Y.; Ivanov, A.I.; Fomina, O.A. (2016) Use of coal-mining and processing wastes in production of bricks and fuel for their burning. *Procedia Eng.* 150, 1496 – 1502. <https://doi.org/10.1016/j.proeng.2016.07.089>.
8. Kusin, F.M.; Munirah, S.N.; Hasan, S.; Hassim, M.A.; Molahid, V.L.M. (2020) Mineral carbonation of sedimentary mine waste for carbon sequestration and potential reutilization as cementitious material. *Environ. Sci. Pollut. Res.* 27, 12767–12780. <https://doi.org/10.1007/s11356-020-07877-3>.
9. Lemougna, P.N.; Yliniemi, J.; Adediran, A.; Luukkonen, T.; Tanskanen, P.; Finnilä, M.; Illikainen, M. (2021) Synthesis and characterization of porous ceramics from spodumene tailings and waste glass wool. *Ceram. Int.* 47 [23], 33286–33297. <https://doi.org/10.1016/j.ceramint.2021.08.231>.
10. Adediran, A.; Lemougna, P.N.; Yliniemi, J.; Tanskanen, P.; Kinnunen, P.; Roning, J.; Illikainen, M. (2021) Recycling glass wool as a fluxing agent in the production of clay- and waste-based ceramics. *J. Clean. Prod.* 289, 125673. <https://doi.org/10.1016/j.jclepro.2020.125673>.
11. Rubin, J.A. (2019) The influence of material and technological factors on radon exhalation from concrete with a cement matrix. Monograph. Publishing house of the Silesian University of Technology. Gliwice, 2019.
12. Gawor, L. (2014) Coal mining waste dumps as secondary deposits – examples from the Upper Silesian Coal Basin and the Lublin Coal Basin. *Geol. Geophys. Environ.* 40 [3], 285–289. <https://doi.org/10.7494/geol.2014.40.3.285>.
13. Abramowicz, A.; Rahmonov, O.; Chybiorz, R. (2021) Environmental management and landscape transformation on self-heating coal-waste dumps in the Upper Silesian Coal Basin. *Land.* 10, 23. <https://doi.org/10.3390/land10010023>.
14. Szczepanska-Plewa, J.; Stefaniak, S.; Twardowska, I. (2010) Coal mining waste management and its impact on the groundwater chemical status exemplified in the Upper Silesia Coal Basin (Poland). *Pol. Geol. Inst. Spec. Pap.* 441, 157–166.
15. Fecko, P.; Tora, B.; Tod, M. (2013) Coal waste: handling, pollution impacts and utilization. The coal handbook: towards cleaner production: Volume 2: Coal Utilisation.
16. Murzyn, P.; Pyzalski, M. (2018) Characteristics and assessment of the suitability of coal-rich mining waste in the production of ceramic building materials. *Multidisc. J. Waste Resour. Resid.* 1, 30-37. <https://doi.org/10.26403/detritus/2018.20>.
17. Council Directive 2013/59/Euratom of 5 December 2013 laying down basic safety standards for protection against the dangers arising from exposure to ionising radiation, and repealing Directives 89/618/Euratom, 90/641/Euratom, 96/29/Euratom, 97/43/Euratom and 2003/122/Euratom.
18. Klinkenberg, L.J. (1941) The permeability of porous media to liquids and gases. American Petroleum Institute, Drilling and Production Practices, Dallas, 200-213.
19. Leonardi, F.; Bonczyk, M.; Nuccetelli, C.; Wysocka, M.; Michalik, B.; Ampollini, M.; Tonnarini, S.; Rubin, J.; Niedbalska, K.; Trevisi, R. (2018) A study on natural radioactivity and radon exhalation rate in building materials containing NORM residues: preliminary results. *Constr. Build. Mater.* 173, 172-179. <https://doi.org/10.1016/j.conbuildmat.2018.03.254>.
20. Sahoo, B.K.; Mayya, Y.S. (2010) Two dimensional diffusion theory of trace gas emission in soil chamber for flux measurements. *Agric. For. Meteorol.* 150, 1211-1224. <https://doi.org/10.1016/j.agrformet.2010.05.009>.